Est. 1984

**ORIENTAL JOURNAL OF CHEMISTRY**
An International Open Free Access, Peer Reviewed Research Journal

www.orientjchem.org

ISSN: 0970-020 X
CODEN: OJCHEG
2017, Vol. 33, No.(5):
Pg. 2271-2281

# Co-sensitized $TiO_2$ Photoelectrodes by Multiple Semiconductors (Pbs/$Pb_{0.05}Cd_{0.95}S$/Cds)to Enhance the Performance of a Solar Cell

**SUPRIYONO[1,2*], AHMAD ZAKARIA[1], YUNI KRISYUNINGSIH KRISNANDI[2] and JARNUZI GUNLAZUARDI[2]**

[1]Department of Chemical Analysis, Politeknik AKA Bogor, Bogor 16154, Indonesia.
[2]Department of Chemistry, Faculty of Mathematics and Sciences,
Universitas Indonesia, Depok 16424, Indonesia.
* Corresponding author E-mail: supriyono272@gmail.com

http://dx.doi.org/10.13005/ojc/330515

(Received: May 13, 2017; Accepted: August 05 , 2017)

**ABSTRACT**

The effect of PbS/$Pb_{0.05}Cd_{0.95}S$/CdS co-sensitization on the quantum dot-sensitized solar cell performance have been investigated. In this research, a $TiO_2$ nanoparticles was prepared by a sol gel method and immobilized to the FTO (fluorine tin oxide) substrate by dip coating technique. The formation of PbS, $Pb_{0.05}Cd_{0.95}S$, and CdS quantum dots (QDs) sensitized $TiO_2$ photoelectrode was carried out by successive ionic layer adsorption and reaction (SILAR) method. The as-prepared materials were characterized by scanning electron microscopy, energy dispersive spectroscopy, X-ray diraction, and X-ray photoelectron spectroscopy. Our photoelectro chemical evaluation indicated that the photocurrent of PbS/$Pb_{0.05}Cd_{0.95}S$/CdS multiple semiconductor (0.363 mA/cm$^2$) is higher than the CdSsingle sensitizer (0.190 mA/cm$^2$), resulting an increase in a photocurrent of 91%. Under 3.5 mW/cm$^2$ illumination, we found that this photoelectrodes have an optimum short-circuit photocurrent density ($I_{sc}$) of 0.429 mA/cm$^2$ and energy conversion eciency of 1.42%, which is 160% higher than that of a CdS single sensitizer (0.54%). The excellent photoelectro chemical properties of our photoanode, suggest that the $TiO_2$ lms co-sensitized by PbS/$Pb_{0.05}Cd_{0.95}S$/CdS quantum dots have potential application in a solar cells.

**Keywords:** Solar Cell, Quantum Dots, SILAR Method, Co-sensitization.

## INTRODUCTION

Increasing demand for energy is forcing us to seekinto an alternative new resources. Among many available candidates, solar energy is ideal to meet the target because of its abundant, clean, and inexhaustible characteristics. Recently, quantum dot-sensitized solar cells (QDSSCs) have received much attention for alternative of dye-sensitized solar cells (DSSCs) owing to their bandgap tune ability, higher absorption coefficient of quantum dots compared to dye molecules, and the ability of multiple-carrier generation[1-4]. However, the efciency of QDSSCs islower compared with other type DSSCs, which restricts their potential application. Thus it is still a crucial issue to enhance itsefciency.

A typical QDSSC, just like DSSC, consists of a QDs-sensitized $TiO_2$ lm photoanode, a redox electrolyte, and a platinized counter electrode[5-6]. As an important component, the photoanode plays a role in the separation of photogenerated charge carriers and the transportation of electrons. $TiO_2$ lms have been demonstrated to be promising candidate as photoanodes due to their appropriate energy band position and both thermal and chemical stability in solution. However, the large band gap of $TiO_2$ (3.2 eV) limits its absorption only to the ultraviolet region, which takes only 3 -5% of the whole solar spectrum reaches earth surfaces.

To improve the performance of QDSSCs, various nanostructures have been employed to fabricate the photoanodes, such as mesoporous lms[7–9], hierarchical sphere[10], nanowires (NWs), nanorods (NRs) and nanotubes (NTs) arrays. Recently, many new strategies, especially the surface and interface treatment, were also employed to modify the nanostructures of the photoanodes, aiming to reduce the recombination and improve the transport of the photo-excited carriers at the interface[10]. To extend the activity of a photoelectrode into the visible light region, various approaches were employed including doping $TiO_2$ with other impurities, using dye-sensitized solar cells (DSSCs), and very recently using the composite semiconductors such as QD s-sensitized solar cells (QDSCs)[11-13].

Many kinds of small bandgap semiconductors that can absorb light in the visible region, e.g., CdS[13], PbSe[14], CdSe[15], InP[16], and CdTe[17], have been used as sensitizers. Among them,CdSis semiconductor with direct band gap ($E_{gap}$) of 2.25eV, which means CdS can trigger wider light absorption range compared to $TiO_2$. However, to accelerate charge separation in bulk/single crystal material, the level of the conduction band (CB) edge which provides the electron injection driving force from QDs to $TiO_2$ should be taken into account. It is known that CdS hasa high CB edges with respect to that of $TiO_2$, and a higher electron injection eciency of CdS was found[18]. PbS is also fascinating sensitizer for QDSSC. The bulk bandgap of PbS (0.41 eV) can be easily manipulated by changing the particle size. The poor stability of PbS quantum dots is a major drawback for QDSSC application. Thus in order to solve the problem, CdS shells are coated on the PbS sensitizer to prevent the corrosion by the polysulfide electrolyte and suppress the recombination at the semiconductor/ electrolyte interface[19-21]. Different from the dye molecules, quantum dot sensitizers may have defects or dislocation. Therefore, enhancing the quality of the quantum dots is an important issue for optimizing QDSSCs[22].

In this study, we prepared $TiO_2$ photo anodesensitizedby multiple semiconductors, which include PbS, $Pb_{0.05}Cd_{0.95}S$, CdS and assembled it into a typical QDSSC. The effect of addinga layer ofquantum dot/sensitizerto the value ofthe photo current and efficiency of the solar cells, then was investigated and will be discussed herein.

## MATERIALS AND METHODS

### Materials

All chemicals and solvents used in this study were of reagent grade. Titanium (IV) isopropoxide, polyethylene glycol (Mr = 1000), triethanolamine, $H_2PtCl_6$, sulphur were purchased from Sigma Aldrich. While methanol, ethanol,2-propanol,$Cd(CH_3COO)_2.2H_2O$,$Na_2S.9H_2O$, $Pb(NO_3)_2$, KCl were purchased from Merck. Distilled water produced from a BioPure purification system was used throughout the experiments and homemade FTO (75X25X1,4 $mm^3$, sheet resistance =21&Ω/sq) were made byspraypyrolysismethod[23].

### Instrumentation

XRD patterns of the prepared film were conducted on X-ray Diffractometer XRD 7000 Shimadzu Cu Ka radiation (l= 0.15418 nm) that operated at 40 kV and 30 mA. FESEM images were taken using FESEM (FEI-Inspect F50). The percentage of elemental composition in the composite film was obtained from energy dispersive spectroscopy (EDSApollo X).The oxidation state of titanium, cadmium, lead, sulfur, and platinum were examined using Thermo VG Scientific-Sigma Probe X-ray photoelectron spectroscopy (XPS) with mono-chromated Al Kα radiation and operating pressure in the sampling chamber was below $5 \times 10^{-9}$ Torr. Photocurrent was measured by electrochemical workstation with a three-electrode configuration, which was connected to a computer-

controlled potentiostat (e-DAQ/e-recorder 401) to record the generated photocurrent. $TiO_2$ photoanode was placed as working electrode, while a Pt wire and Ag/AgCl was placed as counter and reference electrode, respectively. The supporting electrolyte was $Na_2S$0.1M. As source of visible irradiation is 60W wolfram lamp with the intensity 2.20 mW/ $cm^2$.Solar cells performance evaluation was measured by Edaqpotensiostat connected with e-recorder 401.

**Procedure**

**Preparation of FTO/$TiO_2$ film**[24]

Titanium tetraisopropoxide (TTIP), polyethylene glycol (PEG,Mr=1000), triethanolamine, ethanol, FTO (fluorine tin oxide) and distilled water were used in this experiment. $TiO_2$ sol was prepared by mixing of 7.5 ml TTIP, 2.4 ml triethanolamine, and 36 ml of ethanol. The mixture was stirred with a magnetic stirrer at room temperature for 1.5 h, then was added by adequate ethanol-water (4.5:0.5) and 2 g of PEG, and stirred with a magnetic stirrer for 1.5 hours. The resulting sol then was used to coat the FTO glass by a dip coating method, and then annealed at 500°C for 1 hour. This step was repeated 5 timesto obtain $TiO_2$ film on the FTO surface (FTO/$TiO_2$).

**Preparation of FTO/$TiO_2$/CdS Film**

CdS quantum dot (QD) was prepared by a SILAR (successive ionic layer adsorption and reaction) method. Individual solution containing $Cd(CH_3COO)_2$ and $Na_2S$ were used as a Cd and S precursor to obtain CdS quantum dot. The CdS was deposited directly by immersing the FTO/$TiO_2$ glass into an aqueous solution of $Cd(CH_3COO)_2$0.3M for 2 min, then rinsed with distilled water. Then was immersed in aqueous solution of $Na_2S$0.1M for 2 minutes, then rinsed with distilled water. This step was repeated 10 times until the optimum CdS layer was formed. The CdS layer on FTO/$TiO_2$ surface then was dried at room temperature for few minute to obtain FTO/$TiO_2$/CdS film.

**Preparation of FTO/$TiO_2$/PbS/CdS Film**

PbS was prepared by a SILAR (successive ionic layer adsorption and reaction) method.The FTO/$TiO_2$was soaked in the solution of $Pb(NO_3)_2$ 0,02M in methanol for 2 min. and then rinsed with ethanol. Then was soaked in a solution of $Na_2S$0, 01M in methanol: water (1:1) for 5 min., then rinsed with ethanol. This step was performed up to three cycles in order to obtain desired thickness. Then proceed with the Cd Slayerin the same manneras above. The FTO/$TiO_2$/PbS film was immersed into an aqueous solution of $Cd(CH_3COO)_2$0.3M for 2 min, then rinsed with distilled water. Then was immersed in aqueous solution of 0.1M $Na_2S$ for 2 min, then rinsed with distilled water. This step was repeated 10 times until the optimum CdS layer was formed. The CdS layer on FTO/$TiO_2$/PbS surface then was dried at room temperature for few minute to obtain FTO/$TiO_2$/PbS/ CdS film.

**Preparation of FTO/$TiO_2$/PbS/ $Pb_{0.05}Cd_{0.95}S$ /CdS Film**

The FTO/$TiO_2$was soaked in the solution of $Pb(NO_3)_2$ 0,02M in methanol for 2 min. and then rinsed with ethanol. Then was further soaked in a solution of $Na_2S$0,01M in methanol:water (1:1) for 5 min, then rinsed with ethanol. These steps were done in three repeating cycles in order to obtain desired thickness.Then proceedwiththe $Pb_{0.05}Cd_{0.95}$ Slayerusing SILAR method. First, a solution of Pb/ Cd 0,02M in methanol (with a molar ratio of Pb/Cd = 5/95) was prepared by mixing a solution of $Pb(NO_3)_2$ and $Cd(CH_3COO)_2$[24]. QD deposition was performed with SILAR method, firstlyit was soaked in a solution of Pb/Cd 0,02M for 2 min, then rinsed with ethanol. Then it was soaked in a solution of $Na_2S$0,01M for 5 min, then rinsed with ethanol. This step was performed up to threecycles in order to obtain the desired thickness. Then it was proceed with the CdSlayerin the same manneras above to obtain FTO/$TiO_2$/PbS/$Pb_{0.05}Cd_{0.95}$S/CdS film

**Characterization**

Characterization of the film structure was done by using X-ray diffractometer (Shimadzu XRD 7000) with CuK$\alpha$ radiation ($\lambda$ = 1.5418 Å), at 30 kV, 10 mA. Film thickness and morphology of the film surface was observed with FESEM (FEI-Inspect F50). The composition of the constituent elements measured by Energy Dispersive Spectroscopy (Apollo X).The oxidation states of constituent elements were examined by X-ray photoelectron spectroscopy. Photocurrent response was measured using anelectrochemical workstation (e-DAQ/e-recorder 401) using 60W wolfram lamp

as visible light source. Ag/AgCl electrode was used as a reference electrode, while platinum (Pt) was used as a counter electrode and $Na_2S0$,1M as an electrolyte. Photocurrent measurements using multipulse amperometry with a potential = 0 volts and scan time = 100 second.

**Performance Evaluation**

Performance evaluationwas done by using Edaqpotensiostat connected with e-recorder 401. $TiO_2$photoanode was placed as a solar cell working electrode and FTO/Pt was placed as counter electrode. Redox couples $Na_2S$0.2M, S 1M, KCl 0.02M solution was used as an electrolyte and 150W halogen lamp (3.50 mW/cm$^2$ was measured by lux meter) was used as irradiation sources. Isc(short circuit current), and Voc(open circuit voltage) was measured by linear sweep voltammetry (LSV) with scan rate of 40 mV/s from 500 mV to 0 mV under visible illumination.

After solar cells have been fabricated, it should be evaluated for a number of parameters which provide its performance information. These include Isc (short circuit current, mA/cm$^2$), Voc (open circuit voltage, mV), FF (fill-factor) and h (power conversion efficiency). Based on I–V curve, the ll factor (FF) is dened as :

where Im (mA/cm$^2$) and Vm(mV) are the photocurrent and photovoltage for maximum power output (Pm, mW/cm$^2$), The overall energy conversion efciency(h)is defined as:

$$FF = \frac{Pm}{IscxVoc} \quad (1)$$

$$Pm = Im \times Vm \quad (2)$$

$$\eta = \frac{Pm}{pin} \times 100 \quad (3)$$

$$\eta = \frac{Isc \times Voc \times FF \times 100}{pin} \quad (4)$$

$$FF = \frac{k\lambda}{\beta \cos \theta} \quad (5)$$

where Pin (mW/cm$^2$) is the power of incident light

## RESULTS AND DISCUSSION

### Preparation and characterization of the nanostructured $TiO_2$ photoanode

### Composition and crystal structure of the nanostructured $TiO_2$ photoanode

Based on patterns of X-ray diffraction in Fig. 1a, it appears that FTO has a value of 2θ = 26.4°, 33.7°, 37.7°, 51.6°, 54.4°, 61.6°, 64.8° and 65.7° with the indexes Miller (110), (101), (200), (211), (220), (310), (112), and (301). This shows that according to JCPDS 41-1445,our FTO has cassiterite structure . After FTO coated with $TiO_2$, it appears the new peaks at 25.3° and 47.9° and the other peak with increased intensity in 37.8° (Fig. 1b). This corresponds to JCPDS 21-1272, thus it can be concluded that our $TiO_2$ has crystallite structure of anatase.

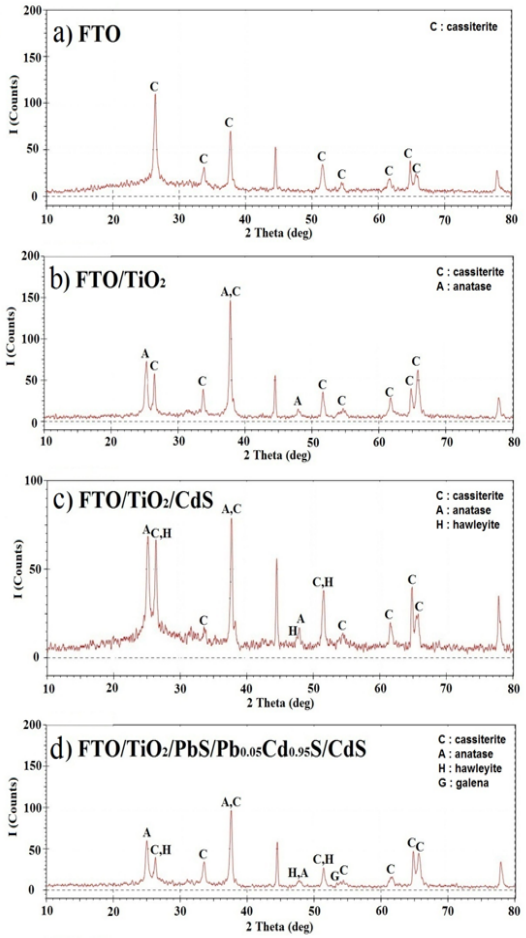


**Fig. 1. X-ray diffraction patterns of $TiO_2$ nanostructured photoanode**

The anatase crystallite size of $TiO_2$ was estimated using the Scherrer equation.where the constant k is a shape factor usually ~ 0.9, $\lambda$ is the wave length of X-ray (0.15418 nm), $\beta$ is the FWHM in radians and $\theta$ is the Bragg's angle.The estimation showsthat the mean crystallyte size of the anatase $TiO_2$ individual particles calculated from Eq. (5) is 22–50 nm.While the dominant peak of rutile $TiO_2$ at 27.4$^O$, 36.1$^O$ and 54.3$^O$ (JCPDS 21-1276) are not visible at all.From XPS spectra,useful information was obtained to assign the complete chemical composition of the sample surface. The survey spectrum in Fig. 2a gives XPS prole of the as-synthesized $TiO_2$ nanoparticles.

The constituents peaks were identied to be titanium (Ti), oxygen (O) and carbon (C). The X-ray photoelectron spectroscopy (XPS) spectra were analyzed for the $TiO_2$ lm in order to study the surface composition of the $TiO_2$ thin lm. The $Ti2p_{3/2}$ and $Ti2p_{1/2}$ spin-orbital splitting photoelectrons for $TiO_2$ (Fig. 2b) are located at binding energies of 458.7 and 464.5 eV, respectively, which is consistent with the values of $Ti^{4+}$ in the $TiO_2$ lattices, as observed earlier by Hung, *et al.*[25]. According to the literature, the $Ti2p_{3/2}$ binding energy of $TiO_2$ is in the range of 458.7–459.2 eV, while the binding energy of titanium in the oxidation state 3+ is in the range of 456.2–457.4 eV[26]. Therefore, titanium exists on the surface in the form of $TiO_2$ with oxidation state 4+. The photoelectron spectra of O1s can be deconvoluted into two peaks (Fig. 2c). The O1s main peak at 529.9 eV is assigned to the metallic oxides, which is consistent with the binding energy of $O^{2-}$ in the $TiO_2$ lattices. A shoulder to the main O1s peak can be observed at high binding energy, 531.8 eV which can be attributed to the hydroxyl groups or chemisorbed water molecules adsorbed on $TiO_2$ surface. In addition, it also shows the presence of C peak (Fig. 2d) at 285.1, 286.8 and 288.6 eV. The deconvolution of the C1s peaks indicates the presence of two peaks at 286.3 and 288.8 eV other than the main peak of sp2-carbon at 284.6 eV. The peaks at 286.3 and 288.8 eV can be attributed to hydroxyl carbon (C–OH) and carboxyl carbon (O=C–O), respectively[27]. This indicates that there are more carbon-containing residues on the lms.This residues were suspected from uncompleted combustion of PEG molecules during calcination.

After CdS deposited on the surface of $TiO_2$, it appears a different X-ray diffraction patterns. In the Fig 1c, it appears that the peak 26.4$^o$ and 51.6$^o$ increased in intensity and appears a small peak at 47.4$^o$. This shows that the CdS has successfully synthesized by SILAR method and according to JCPDS 10-0454, this CdS has hawleyite crystallite structure. The small intensity of CdS peaks was caused by asmall quantities of CdS deposited on the $TiO_2$ surface. It was only about 1: 6 (Cd: Ti), as shown in the EDS spectrum in fig. 3.b. According to Balaz, *et al.*[28], CdS has two structures, these are hexagonal $\alpha$-CdS called greenockite (JCPDS 41-1049) and cubic $\alpha$-CdS called hawleyite (JCPDS 10-0454). Our CdS is in accordance with the

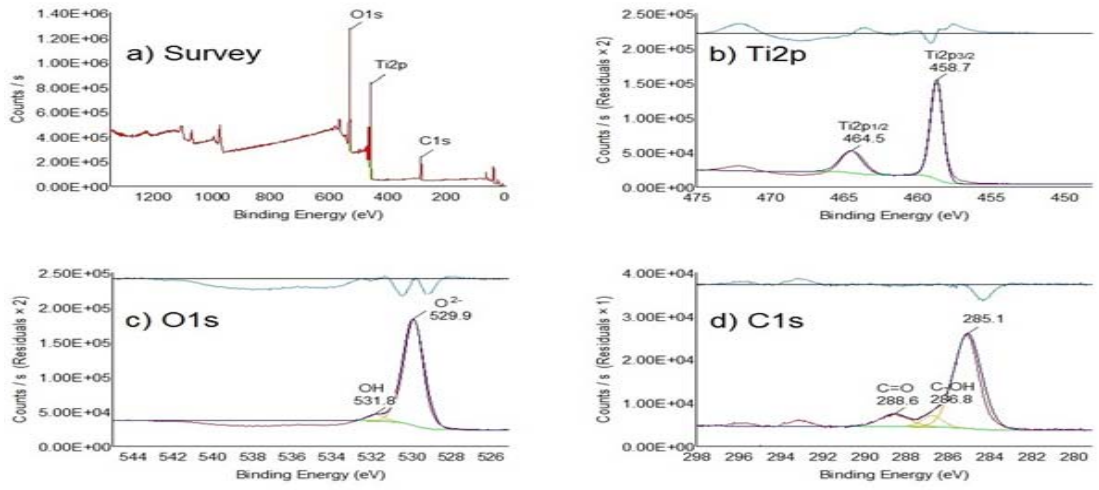


**Fig . 2 . XPS spectrum of FTO/$TiO_2$ thin film**

hawleyite structure. Besides coated by CdS, $TiO_2$ is also coated by PbS. Characterization of FTO/$TiO_2$/PbS/$Pb_{0.05}Cd_{0.95}S$/CdS layer with X-ray diffraction does not show any clear PbS peaks. Only a small peak seen in 53.4° (Fig. 1d), this due to the amount of PbS deposited on the $TiO_2$ surface is very small, only about 1:12 (Pb : Ti) as shown in the EDS spectrum in Fig 3c. Beside that reason, PbS and CdS layer is only dried at room temperature with out any calcination, so likely PbS and CdS still have an amorphous structure and the resulted peak tends to be broaden. PbS has only a galena single crystal structure, so it can be ascertained that our PbS has galena structure (JCPDS 05-0592).

The spectrum of the overall survey scanof FTO/$TiO_2$/PbS/$Pb_{0.05}Cd_{0.95}S$/CdS thin layer (Fig. 4a)indicates the presence of Ti, O, Pb, Cd, and S in the sample. The $Cd3d_{5/2}$ and $Cd3d_{3/2}$ binding energies are equal to 405.0 eV and 411.8 eV (Fig 4b) and it corresponds to $Cd^{2+}$.

For cadmium sulde, the $Cd3d_{5/2}$ binding energy is in the range of 404.4 – 405.7 eV[29]. Fig. 4d shows XPS spectra of S2p levels of CdS nanoparticles. S2p

peaks observed at 161.3 eV (for $S2p_{3/2}$) and 162.7 eV (for $S2p_{1/2}$) are attributed to metal sulde. Observed values of the $S2p_{3/2}$ binding energy for sulfur in the suldes is in the range of 161.1–161.7 eV[29]; sulfates and sultes are characterized by the higher S2p binding energy in the range of 168–170 eV[30]. The resolution of the XPS spectra of the Pb resulted in peaks at different binding energies. The $Pb4f_{7/2}$ and $Pb4f_{5/2}$ spin-orbital splitting photoelectrons for PbS (Fig. 4c) are located at binding energies of 138.2 eV and 142.9 eV, respectively, which is consistent with the values of $Pb^{2+}$ in the PbS lattices[31]. In addition, it also shows the presence of C peak (Fig. 4e) as well as O peak (Fig 4f) at 285.0 and 530.0 eV, respectively, as impurities. The O1s main peak at 530.0 eV is assigned to the metallic oxides, which is consistent with the binding energy of $O^{2-}$ in the $TiO_2$ lattices. A shoulder to the main O1s peak can be observed

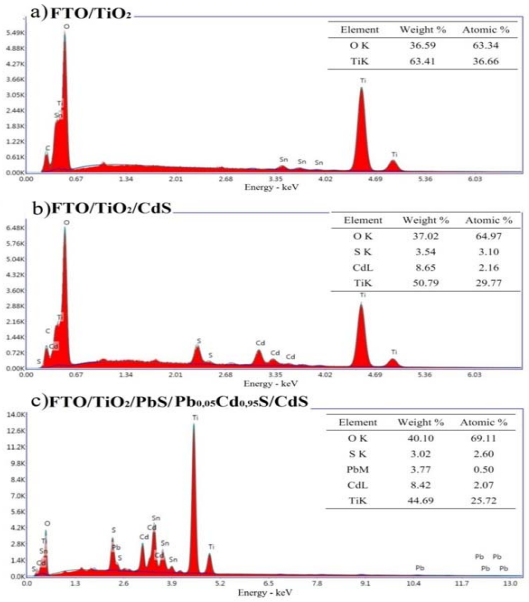


**Fig. 3 . EDS spectrum and elemental composition of $TiO_2$ nanostructured photoanode**

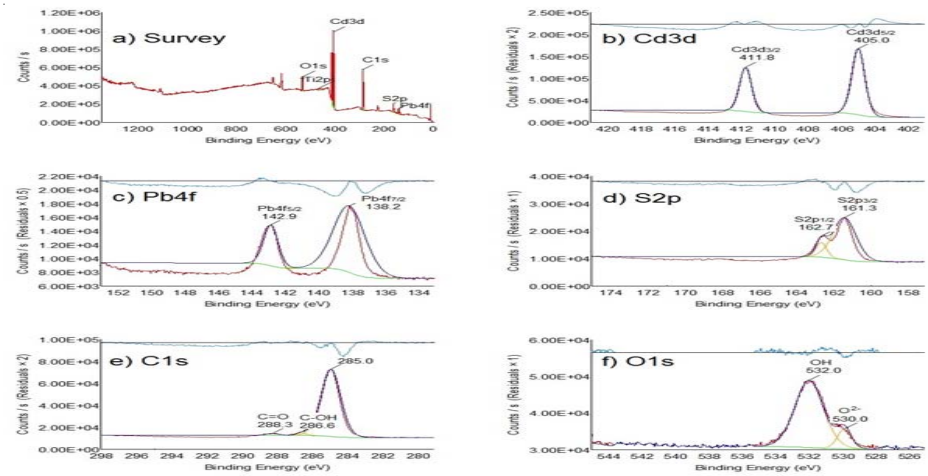


**Fig. 4 . XPS spectrum of FTO/$TiO_2$/PbS/$Pb_{0.05}Cd_{0.95}S$/CdS thin films**

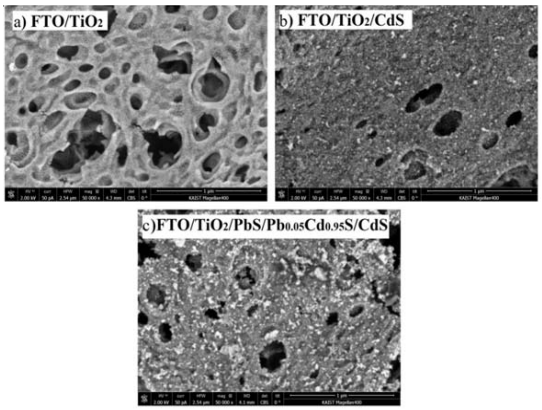


**Fig. 5. SEM images of $TiO_2$ nanostructured photoanode**

at higher binding energy, 532.0 eV which can be attributed to the hydroxyl groups or chemisorbed water molecules adsorbed on $TiO_2$ surface. The deconvolution of the C1s peaks indicates the presence of two peaks at 286.3 and 288.8 eV other than the main peak of sp2-carbon at 284.6 eV. The peaks at 286.3 and 288.8 eV can be attributed to hydroxyl carbon (C–OH) and carboxyl carbon (O=C–O), respectively. This peaks were suspected from uncompleted evaporation of methanol / ethanol solvent used in $Pb^{2+}$ and $S^{2-}$ solution.

### Surface morphology of the nanostructured $TiO_2$ photoanode

From Fig.5a shows that the $TiO_2$ deposited on the surface of the FTO, has a porous structure with a diameter of less than 1 µm. Pores are from PEG template that lost during calcination. Pores are useful to hold sensitizer in larger quantities. CdS and PbS will fill the pores of $TiO_2$ so that these pores will be full after the sensitizer enter into it, as shown in Fig 5b & 5c. But in wide pores, sensitizer only able to coat the inner walls of the pores so that the pores are still open with a smaller diameter (Fig. 5c). PbS and CdS largely occupy space in the pores and only a few of this sensitizer which occupies on the surface of $TiO_2$. This reason is supported by a cross-sectional images in Fig 6, that thethickness of $TiO_2$/PbS/$Pb_{0.05}Cd_{0.95}S$/CdS layer is only slightly thicker than the $TiO_2$ layer.

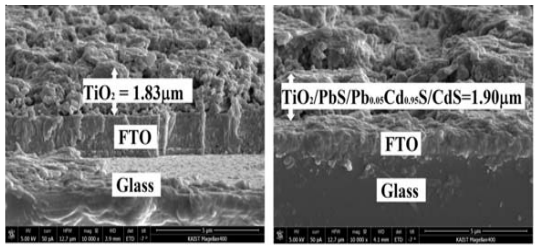


**Fig. 6. Cross-sectional SEM images of $TiO_2$ nanostructured photoanode (a) FTO/TiO2, (b) FTO/TiO2/PbS/$Pb_{0.05}Cd_{0.95}S$/CdS**

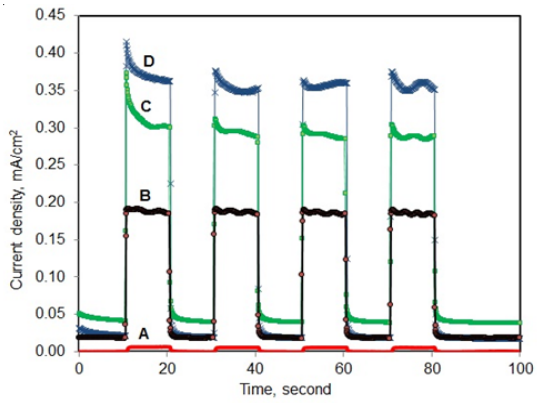


**Fig. 7 .The photocurrent of $TiO_2$ nanostructured photoanode A)FTO/$TiO_2$, B)FTO/$TiO_2$ /CdS, C)FTO/ $TiO_2$/PbS/CdS, D)FTO/$TiO_2$/PbS/$Pb_{0.05}Cd_{0.95}S$/CdS (illuminated with 60W wolfram lamp, 2.20 mW/cm$^2$; electrolyte =$Na_2S$ 0.1M, bias potensial = 0 Volt).**

### Photoelectro chemical response of the nanostructured $TiO_2$ photoanode

Light absorption, particularly in the visible region, can be increased by using a narrow bandgap quantum dots. Two or more different band gap quantum dots can be used at a same time so that the light is not absorbed by the first quantum dot, can still be absorbed by the second quantum dot. This phenomenon is called as co-sensitization, the sensitization was carried out by two or more sensitizers. With the co-sensitization makes the larger absorption of the incident light. The more light is absorbed, the more likely the resulting photocurrent. In this study two sensitizers, CdS and PbS were used. CdS has a bandgap 2.25 eV coupled with PbS which has a band gap of 0.41 eV. CdS has absorption in the visible region is at a wavelength of 550 nm while PbShas absorption in the infra red region ($\pm$ 3000nm). With the merger of two quantum dot, it is expected to increase the

absorption of visible light so that it will increase its photocurrent. From the observation of the photocurrent in Fig. 7, it is clear that the two sensitizer PbS and CdS able to improve the higher photocurrent.

Mixture of PbS and CdS, is $Pb_{0.05}Cd_{0.95}S$ which has a bandgap between them, was able to increase the absorption in the visible region and simultaneously improve its photocurrent. FTO/$TiO_2$/ Cd Slayer generates a photocurrent of about 0.190 mA/cm$^2$ while FTO/$TiO_2$/PbS/CdS about 0.302 mA/cm$^2$, so that the PbS able to increase the photocurrent of 59%. The existence of $Pb_{0.05}Cd_{(0.95}S$ layer between PbS and CdS layer is useful to accelerate the transfer of electrons from CdS layer to PbS. FTO/$TiO_2$/PbS/ $Pb_{0.05}Cd_{0.95}S$ /CdS layer able to generate photocurrent up to 0.363 mA/cm$^2$. Therefore, combination of PbS and $Pb_{0.05}Cd_{0.95}S$ layer able to increase the photocurrent up to 91%.

The mechanism of electron flow is highly dependent on the position of the conduction band of each semiconductor. CdS semiconductor which has a conduction band edge of -4.0 eV is estimated as the beginning of a flow of electrons. CdS with the bandgap 2, 25eV will be excited when exposed by the light with a wavelength smaller than 550 nm. From the CdS conduction band, the electrons will flow into the conduction band PbS of -4.1 eV. In addition to receive an electrons from CdS, PbS semiconductor can also be a source of electrons. PbS with a band gap of 0.41 eV will be excited when exposed by the light with a wavelength of less than 3000nm. Electrons from the Pb Svalence band will move toward the Pb Sconduction band. Further more, from the Pb Sconduction band, electrons proceed to the $TiO_2$ conduction band of -4.2 eV. From the $TiO_2$ conduction band, the electrons move toward the $SnO_2$conduction band of -4.8 eV, to get to the external circuit. Mean while, to prevent electron-hole recombination is required hole transporting material is $S^{2-}$ from the redox electrolyte. For more details of the electrons flow, can be seen in Figure. 8. below

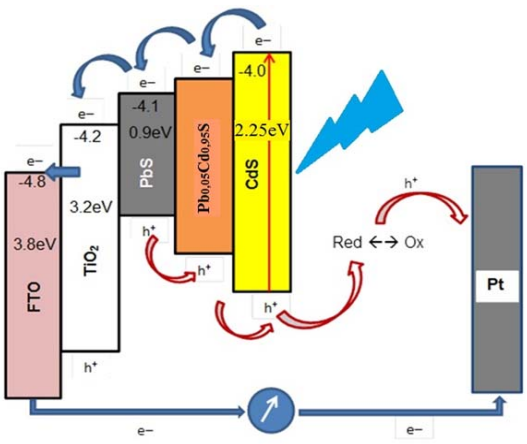


**Fig. 8. Schematic diagram illustrating the electron flow of PbS-CdS co-sensitized solar cells**

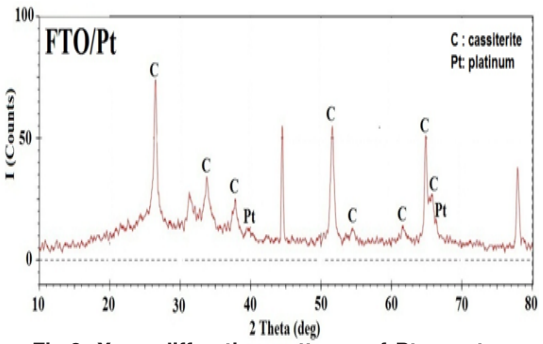


**Fig.9. X-ray diffraction patterns of Pt counter electrode.**

**Preparation of Pt counter electrode**

Pt counter electrode is made by depositing Pt on the surface of the FTO. From X-ray diffraction pattern in Fig. 9, it appears that the metals Pt have been successfully deposited on the surface of the FTO.

It appears from the new peak appearing at 39,4° and 66.4° which is the peak of platinum according to JCPDS 88-2343. The amount of Pt deposited on the surface of the FTO is very small that is around 1:10 (Pt: Sn)as shown in the EDS spectra in Fig. 10, so that the resulted peak in X-ray diffraction pattern has also a small intensity. Although the amount of Pt is very small but platinum crystals have a uniform shape, as shown in Figure 11.

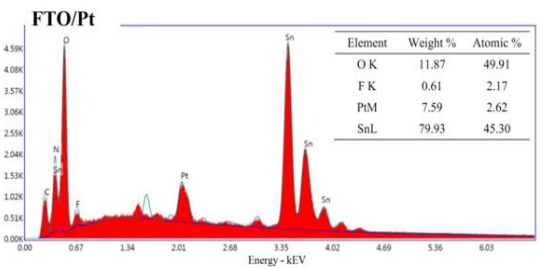


**Fig. 10. EDS spectrum and elemental composition of Pt counter electrode**

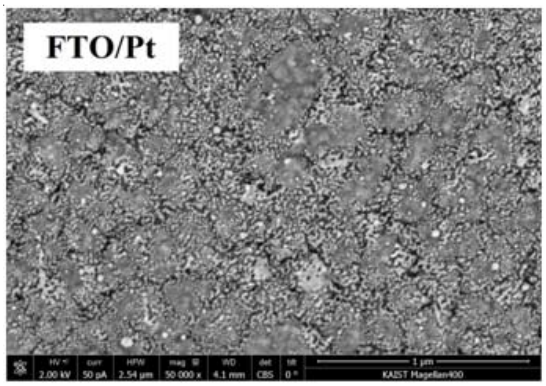


**Fig. 11 . SEM images of Pt couter electrode**

Figure 12a is the typical survey spectrum of FTO/Pt thin lm, showing the presence of Pt, Sn, O and C. The corresponding Pt4f spectra are shown in Fig 12b. It is seen that the $Pt4f_{7/2}$ binding energy is 70.7 eV that is typical of metallic platinum. According to Kalinkin, *et al.*[32], for the chloride complexes, the Pt4f spectrum is shifted to higher binding energies by a value proportional to the oxidation state of platinum. For example, for $K_2PtCl_4$ (the oxidation state of platinum is $Pt^{2+}$) and $K_2PtCl_6$ ($Pt^{4+}$), the binding energy ($Pt4f_{7/2}$) values are 73.1 eV and 75.2 eV, respectively. As a consequence, the shift of the $Pt4f_{7/2}$ photoemission line with respect to that of the metal is 2.0 eV for $Pt^{2+}$ and 4.1 eV for $Pt^{4+}$, i.e. about 1 eV per unit oxidation number. Binding energies of $Sn3d_{3/2}$ and $Sn3d_{5/2}$ electrons in the surface layer of the FTO materials were found to be 494.9 eV and 486.7 eV respectively, which corresponded to $Sn^{4+}$ in the tin dioxide.

**Performance evaluation of the solar cells**

Solar cells was constructed by assembling the working electrode and the counter electrode by using a redox electrolyte $Na_2S/S$. Solar cell performance evaluation was done by using the potentiostat and 150W halogen lamp as a light visiblesource. Intensity of halogen lamp was measured by a lux meter and was obtained the intensity at a distance of 10 cm of 3.50 mW/cm$^2$. From3different configurations are $FTO/TiO_2/CdS$, $FTO/TiO_2/PbS/CdS$, $FTO/TiO_2/PbS/Pb_{0.05}Cd_{0.95}S/CdS$ obtained I-V curves as indicated in Figure 13.

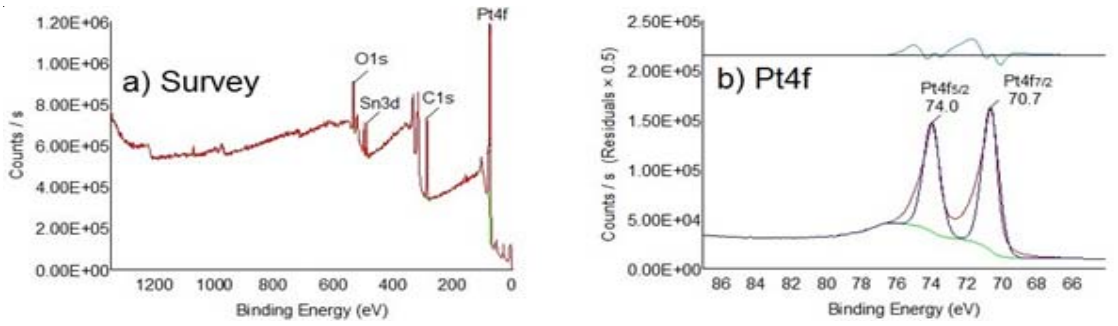


**Fig. 12. XPS spectrum of FTO/Pt thin film**

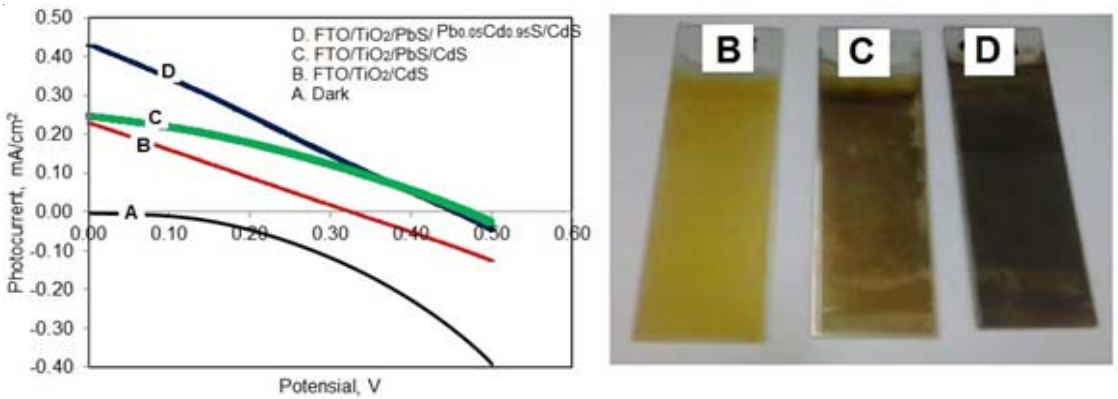


**Fig. 13. Left : I-V curve for performance evaluation of solar cells; Right : Color of $TiO_2$ nanostructured photoanodes as working electrode B)$FTO/TiO_2/CdS$, C)$FTO/TiO_2/PbS/CdS$, D)$FTO/TiO_2/PbS/Pb_{0.05}Cd_{0.95}S/$**

Based on the I-V curve in Fig. 13, it can be determined the value of the fill factor, Isc, Voc, and efficiency, using the formula described above, in order to obtain the following results, as indicated in table. 1.

From the table. 1, it is obtained the efficiency for CdS single sensitizer=0:54% and using (PbS+CdS+$Pb_{0.05}Cd_{0.95}S$)=1.42%. Thus an increase in efficiency of around 160% on solar cells using multiple semiconductor compared with solar cells using a single semiconductor of CdS.

**Table. 1 : The value of the fill factor, $I_{sc}$, $V_{oc}$, and efficiency of solar cells**

| Sensitizer | $I_{max}$ mA/cm² | $V_{max}$ mV | $I_{sc}$ mA/cm² | $V_{oc}$ mV | FF | $P_{max}$ mW/cm² | $P_{in}$ mW/cm² | h (%) |
|---|---|---|---|---|---|---|---|---|
| CdS | 0.1172 | 162 | 0.2298 | 327 | 0.253 | 0.0190 | 3.501 | 0.54 |
| PbS/CdS | 0.1462 | 257 | 0.2446 | 469 | 0.328 | 0.0376 | 3.501 | 1.07 |
| PbS/$Pb_{0.05}Cd_{0.95}S$/CdS | 0.2285 | 217 | 0.4286 | 452 | 0.256 | 0.0496 | 3.501 | 1.42 |

## CONCLUSION

Based on the results obtained, it can be concluded that $TiO_2$ nanostructured photoanode have been successfully prepared by utilizing two semiconductor namely CdS and PbS. Quantum dot of CdS, PbS and $Pb_{0.05}Cd_{0.95}S$ have been successfully prepared using SILAR method and obtained photocurrent of 0.190 mA/cm² for configuration FTO/$TiO_2$/CdS, 0.302 mA/cm² for FTO/$TiO_2$/PbS/CdS and 0.363 mA/cm² for FTO/$TiO_2$/PbS/$Pb_{0.05}Cd_{0.95}S$/CdS. Sensitizers which use multiple semiconductors namely PbS, CdS and $Pb_{0.05}Cd_{0.95}S$ able to increase the photocurrent of 91% greater than that using a single semiconductor of CdS. Based on the incident light of 3.5 mW/cm², the all three types constructed solar cells show efficiency of 0.54%, 1.07% and 1.42%, respectively. It can be concluded that the efficiency has been increase of around 160% when multiple semiconductorsPbS, CdS, $Pb_{0.05}Cd_{0.95}S$ were used.

## ACKNOWLEDGEMENTS

One of the authors (Supriyono) wish to thank to Industrial Education and Training Center, Ministry of Industry of Indonesia for providing the research funding. Partial support from Research Cluster Scheme Universitas Indonesia, and opportunity provided by KAIST (Korean Advanced Institute of Science and Technology) for SEM and XPS measurements are also acknowledged.

## REFERENCES

1. Kamat, P.V.; Tvrdy, K.; Baker, D.R.; Radich, J.G. *Chem. Rev*, **2010**, *110*, 6664.
2. Yu, W.; Peng, X. *Angew. Chem*, **2002**, *41*, 2368.
3. Ruhle, S.; Shalom, M.;Zaban, A. *Chem Phys Chem*, **2010**, *11*, 2290.
4. Semonin, O.E.; Luther, J.M.; Choi, S.; Chen, H.Y.; Gao, J.; Nozik, A.J.; Beard, M.C. *Science*, **2011**, *334*, 1530.
5. Grätzel, M. *Acc. Chem. Res.* **2009**, *42*, 1788.
6. Grätzel, M.*Nature*, **2001**, *414*, 338.
7. Im, S.H.;Lee, Y.H.; Seok, S.I.; Kim, S.W. *Langmuir*, **2010**, *26*, 18576.
8. Yang, Z.;Chen, C.Y.;Liu, C.W.;Li, C.L.;Chang, H.T. *Adv. Energy Mater.* **2011***, 1*, 259.
9. Zhang, Q.; Guo, X.; Huang, X.; Huang, S.; Li, D.; Luo, Y.; Shen, Q.; Toyoda, T.; Meng, Q. *Phys. Chem. Chem. Phys.* **2011**, *13*, 4659.
10. Yu, X.Y.; Liao, J.Y.; Qiu, K.Q.; Kuang, D.B.; Su, C.Y. *ACS Nano*, **2011**, *5*, 9494.
11. Yang, Z.; Chen, C.Y.; Roy, P.; Chang, H.T. *Chem. Commun*, **2011**, *47*, 9561–9571.
12. Lee, Y.L.; Lo, Y.S. *Adv. Funct. Mater*, **2009**, *19*, 604–609.
13. Wang, H.; Bai, Y.S.; Zhang, H.; Zhang, Z.H.; Li, J.H.;Guo, L.J. *Phys. Chem. C*, **2010**, *114*, 16451–16455.
14. Schaller, R.D.; Klimov, V.I. *Phys. Rev. Lett*, **2004**, *92*, 186601.
15. Guijarro,N.; Villarreal, T.L.;Sero, I.M.;Bisquert, J.; Gomez, R.J. *Phys. Chem. C*, **2009**, *113*, 4208–4214.
16. Blackburn, J.L.;Selmarten, D.C.;Ellingson, R.J.; Jones, M.;Micic, O.;Nozik, A.J. *J. Phys. Chem. B*, **2005**, *109*, 2625–2631.

17. Gao,X.F.; Li,H.B.;Sun,W.T.;Chen,Q.; Tang, F.Q.;Peng, L.M. *J. Phys. Chem. C*, **2009**, *113*, 7531–7535.
18. Chi, C.F.; Cho, H.W.;Teng, H.; Chuang, C.Y.; Chang, Y.M.;Hsu, Y.J.; Lee, Y.L. *Appl. Phys. Lett*, **2011**, *98*, 012101.
19. Zhou, N.; Chen, G.; Zhang, X.; Cheng, L.;Luo, Y.; Li, D.; Men, Q. *Electrochem. Commun*, **2012**, *20*, 97.
20. Hachiya, S.; Shen, Q.; Toyoda, T. 2012, *J. Appl. Phys*. **2012**, *111*, 104315.
21. Samadpour, M.;Boix, P.P.;Gimenez, S.;Zad, A.I.;Taghavinia, N.; Mora-Sero, I.;Bisquert, J. *J. Phys. Chem. C*, **2011**, *115*, 14400.
22. Guijarro, N.; Lana-Villarreal, T.;Shen, Q.; Toyoda, T.; Gomez, R. *J. Phys. Chem. C*, **2010**, *114*, 21928.
23. Supriyono;Surahman, H.; Krisnandi, Y.K.; Gunlazuardi, J. *ProcediaEnv. Sci*. **2015**, *28*, 242-251.
24. Supriyono; Krisnandi, Y.K.; Gunlazuardi, J. *Int. J. ChemTech. Res*, **2016**, *9(7)*, 191-198.
25. Hung, W.C.; Chen, Y.C.; Chu, H.; Tseng, T.K. *Appl. Surf. Sci*. **2008**, *255*, 2205-2213
26. Finetti, P.; Sedona, F.; Rizzi, G.A.; Mick, U.; Sutara, F.;Svec, M.; Matolin, V.; Schierbaum, K.; Granozzi, G. *J. Phys. Chem. C*, **2007**, *111,* 869–876.
27. Zhao, Y.; Liu, H.; Wang, F.; Liu, J.; Park, K.C.; Endo, M. *J. Solid State Chem.* **2009**, *182*, 875-880
28. Balaz, P.;Boldizarova, E.;Godocikova, E.; Briancin, J. *Mater. Lett*., **2003**, *57*, 1585-1589.
29. Yang, M.;Shrestha, N.K.;Schmuki, P. *Electrochim. Acta*, **2010**, *55*, 7766–7771.
30. Appay, M.D.;Manoli, J.M.;Potvin, C.;Muhler, M.; Wild, U.;Pozdnyakova, O.;Paal, Z. *J. Catal*, **2004**, *222*, 419-428.
31. Mathews, N.R.; Angeles-Chavezb. C.; Cortes-Jacomeb, M.A.; Antonio, J.A.T. *Electrochim. Acta*, **2013**, *99*, 76-84.
32. Kalinkin, A.V.; Smirnov, M.Y.;Nizivskii, A.I.;Bukhtiyarov, V.I. *J. Electron Spectroscopy and Related Phenomena*, **2010**, *177*, 15-18.